

Chiral Biobased Ionic Liquids with Cations or Anions including Bile Acid Building Blocks as Chiral Selectors in Voltammetry

Sara Grecchi⁺,^[a] Claudio Ferdeghini⁺,^[b] Mariangela Longhi,^[a] Andrea Mezzetta,^[b] Lorenzo Guazzelli,^[b] Siriwat Khawthong,^[a] Fabiana Arduini,^[c] Cinzia Chiappe[#],^[b] Anna Iuliano,^{*[d]} and Patrizia Romana Mussini^{*[a]}

Chiral ionic liquids (CILs), or ionic liquids (ILs) with chiral additives, are very attractive chiral media for enantioselective electroanalysis, on account of their high chiral structural order at the electrochemical interphase. A family of molecular salts with CIL properties is now introduced, based on the chiral steroid building block of deoxycholic acid implemented either in the anion or cation. Testing them as chiral additives in a commercial achiral IL, they enable voltammetric discrimination of the enantiomers of a model chiral probe on disposable

screen-printed electrodes in terms of peak potential differences, which is the most desirable transduction mode of the enantiorecognition event. The probe enantiomer sequence is the same for all selectors, consistent with their sharing the same chiral building block configuration. This proof-of-concept widens the application fields of bile acid derivatives as chiral selectors, while also enriching the still very few CIL families so far explored for applications in chiral electroanalysis.

1. Introduction

Chiral ionic liquids (CILs), a subclass of ionic liquids (ILs), are chiral low melting point organic salts combining the attractive properties of ILs (such as negligible vapor pressure at ambient conditions, good thermal stability, favorable solvation behavior, modulability of functional properties through molecular design, as well as ability to allow for high reactivity and selectivity when used as solvents)^[1,2] with enantiodiscrimination ability in various chiral recognition processes.^[3–7] Very recent studies point to CILs, or even ILs with chiral additives, being of huge

interest as chiral media for enantioselective electrochemistry and electroanalysis, too.^[8–11] Actually, ILs are known to result in much higher and longer-range order at the electrode|solution interphase respect to the double layer structure of “classical” solvent + supporting electrolyte systems,^[12–24] a peculiarity still holding in the presence of significant water amounts,^[18] this feature can be regarded as an attractive tool for achieving high control in electron transfer processes, for both analytical and preparative applications. In particular, in the case of CILs such high order can promote effective transmission of the chiral information. Actually, recent voltammetry studies in CILs or even in ILs modified with chiral molecular additives (which could modulate their local structure at the electrochemical interphase, similarly to the well know effect of chiral additives on bulk liquid crystals)^[25] resulted in the observation of significant potential differences^[8–11] for the enantiomers of chiral electroactive probes on achiral electrodes. As it could be expected, such enantiodiscrimination ability appears to be significantly modulated by the CIL molecular structure (and, in the case of IL + chiral additive systems, by the IL molecular structure as well as by the chiral additive molecular structure and concentration). In particular, large peak potential differences have been observed in ILs with addition of molecular salts with “inherently chiral” cations of axial or helical stereogenicity,^[8,10,11] and either solid or liquid at room temperature; even better performances could be obtained employing the latter ones, inherently chiral ionic liquids (ICILs), as bulk media.^[26] However, the less conspicuous but significant potential differences observed in ionic liquid media with chirality arising from the presence of one or more stereocenters^[9] should be regarded with high interest, too. Indeed, central stereogenicity, which is the most common case, often corresponds to chiral selectors easily affordable and available in large quanti-

[a] S. Grecchi,⁺ Dr. M. Longhi, S. Khawthong, Prof. P. R. Mussini
 Dipartimento di Chimica
 Università degli Studi di Milano
 Via Golgi 19, 20133 Milan, Italy
 E-mail: patrizia.mussini@unimi.it

[b] C. Ferdeghini,⁺ Dr. A. Mezzetta, Prof. L. Guazzelli, Prof. C. Chiappe[#]
 Dipartimento di Farmacia
 Università degli Studi di Pisa
 Via Bonanno 33, 56126 Pisa, Italy

[c] Prof. F. Arduini
 Dipartimento di Scienze e Tecnologie Chimiche
 Università di Roma Tor Vergata
 Via della Ricerca Scientifica 1 00133 Rome, Italy

[d] Prof. A. Iuliano
 Dipartimento di Chimica e Chimica Industriale
 Università degli Studi di Pisa
 Via G. Moruzzi 13, 56124 Pisa, Italy
 E-mail: anna.iuliano@unipi.it

[†] These authors contributed equally to this work.

[#] Deceased

Supporting information for this article is available on the WWW under <https://doi.org/10.1002/celec.202100200>

© 2021 The Authors. ChemElectroChem published by Wiley-VCH GmbH. This is an open access article under the terms of the Creative Commons Attribution License, which permits use, distribution and reproduction in any medium, provided the original work is properly cited.

ties, including many natural compounds that can be advantageously exploited as enantiomerically pure building blocks for the preparation of chiral CILs. Actually, the CILs considered in the above cited paper^[18] consisted in cations with biobased chiral building blocks from natural terpenoids (1*R*)-myrtenol, (*S*)-perillyl alcohol, (1*R*)-nopol, and (*S*)-citronellol, combined with bistriflimide as counter anion, to lower melting points below room temperature.

In this frame, it is quite interesting to comparatively test as media for electroanalysis and electrochemistry CILs that exploit different kinds of chiral biobased building blocks. Of course, the chiral natural compounds used for the synthesis of CILs must possess functional groups that allow for the introduction of suitable moieties both for enantiodiscrimination of interactions and for conversion into salts. Deoxycholic acid, one of the most common and commercially available bile acids, fulfils these criteria: it is characterized by a concave structure endowed with several stereogenic centers of established absolute configuration, two hydroxyl groups, which have different reactivity due to the different steric environment, and a carboxylic acid group in the lateral chain, which can be used for conversion into salt. By virtue of these peculiarities, deoxycholic acid has been successfully used as scaffold for the preparation of different chiral auxiliaries, whose properties not only depend on the introduced moieties, but also on the position of these moieties on the cholestanic backbone. Their use span from the enantioselective chromatography^[27–30] to asymmetric

catalysis^[30–35] and enantioselective synthesis.^[36–38] Despite these interesting characteristics, CILs obtained from deoxycholic acid, and also from other bile acids, are to the best of our knowledge not reported in the literature. Thus, the longstanding experience of some of us in the field of the ionic liquids^[39–43] and in the use of bile acids in chemical enantiodiscrimination processes^[44–51] suggested the synthesis of new CILs starting from deoxycholic acid (Figure 1).

To this aim, the carboxylic group was converted in a good leaving group for the nucleophilic displacement with 1-methylimidazole to obtain CILs having the chiral steroidal cation, or underwent a neutralization reaction to obtain CILs having the steroidal anion. To lower the melting point of the ionic compounds one or two long alkyl chains were introduced, by derivatization of the hydroxyl groups as esters. In addition, an aromatic group was introduced at the two different functionalized positions, which could provide an additional coordination element for chiral recognition.

Thus, respect to the terpenoid-based CIL family formerly tested for chiral electroanalysis,^[9] the present one features extremely bulkier chiral building blocks, with no less than ten stereocenters. It also offers a convenient molecular structure series for a first systematic investigation of features and enantiodiscrimination ability in electrochemistry and electroanalysis, including:

(i) A group of six CILs with the chiral building block implemented in the cation; it includes all combinations of three

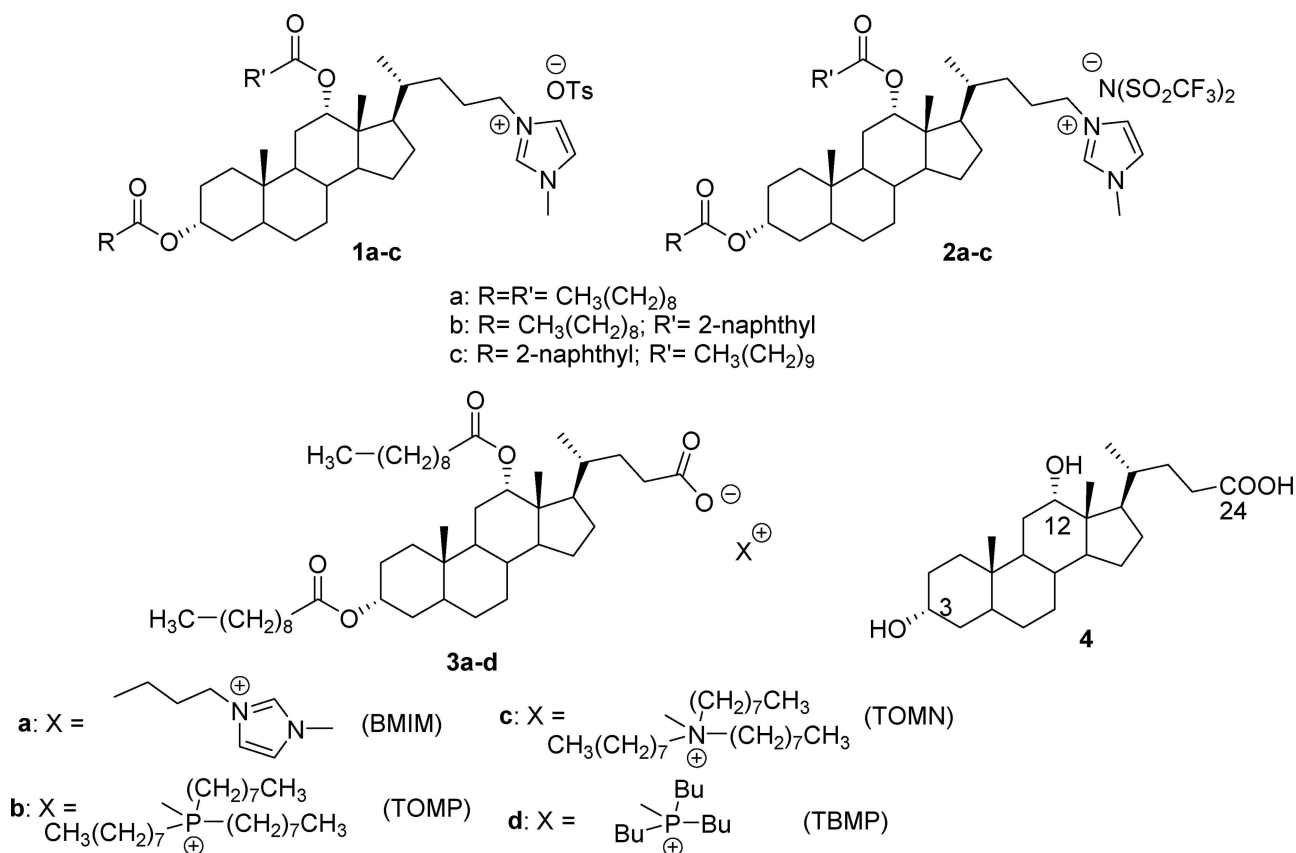


Figure 1. Structure of the synthesized CILs (1–3) and deoxycholic acid (4).

systematically different chiral imidazolium cations (having the same chiral steroid block, with either two long chain esters or one long chain ester and one naphthyl ester substituents) with two different achiral anions: tosylate (OTs) and bistriflimide (NTf₂) (**1a–c** and **2a–c** in Figure 1).

(ii) A group of four CILs with the chiral building block implemented in the carboxylate anion (having in all cases the same chiral steroid block with two decanoyl ester substituents, as in cases **1a** and **2a**) combined with four different cations, *i.e.* 1-butyl-3-methylimidazolium, trioctyl methyl ammonium, trioctyl methyl phosphonium, tributyl methyl phosphonium (**3a–d** in Figure 1).

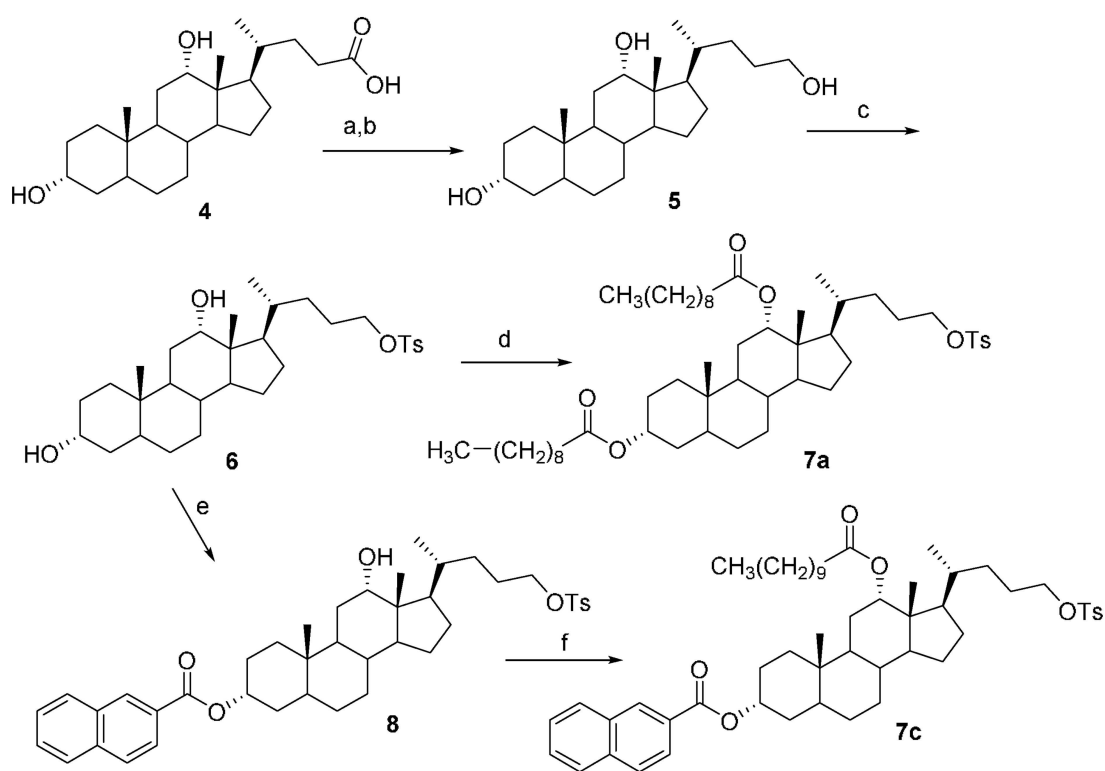
The novel CIL family has been thus characterized concerning key physic-chemical and electrochemical properties and tested as media for enantioselective voltammetry experiments with the enantiomers of a model electroactive chiral probe.

2. Results and Discussion

2.1. Synthesis of the CILs

The general strategy for the synthesis of deoxycholic acid derived CILs with the steroidal backbone in the cationic moiety, involved the introduction of a good leaving group on the lateral

chain, which could be easily displaced by 1-methylimidazole, affording the ionic compound. As reported in Scheme 1, the deoxycholic acid **4** has been reacted with ethylchloroformate giving a mixed anhydride intermediate, which was *in situ* reduced by NaBH₄,^[52] affording the trihydroxycholane **5**. The primary hydroxyl group was converted into the corresponding p-toluensulfonate with high selectivity, by reacting **5** with 1.5 equiv. of p-toluensulfonyl chloride at room temperature. Under these reaction conditions the tosylate **6** was obtained in a 70% yield, after chromatographic purification: it is to note that all the attempts to obtain selectively the corresponding mesylate failed, the product possessing two mesylate groups at 3 and 24 positions being obtained. The esterification of the two secondary hydroxyl groups of **6** with decanoyl chloride was carried out according to a protocol used to derivatize the methyldeoxycholanoate,^[53] which was modified for the reaction temperature. The control of the reaction temperature was crucial: in fact at room temperature only the hydroxyl group at the position 3, which is equatorial, reacted, whereas in refluxing toluene, as in the original protocol, both the hydroxyl groups were derivatized but, at the same time, the displacement of the tosylate group by the chloride ion, present in the reaction mixture, was obtained. Derivative **7a** was obtained in an 83% yield by maintaining the reaction temperature at 50 °C, a good



Reagents and conditions

a: ethylchloroformate, Et₃N, rt, 12 h; **b:** NaBH₄, H₂O, rt, 12 h; **c:** TsCl, Et₃N, THF, rt, 12h; **d:** decanoyl chloride, BTEAC, CaH₂, toluene, 50 °C, 12 h; **e:** 2-naphthoyl chloride, Et₃N, DMAP, rt, 24 h; **f:** undecanoic acid, DCC, DMAP,

Scheme 1. Synthesis of tosylates **7a** and **7c**.

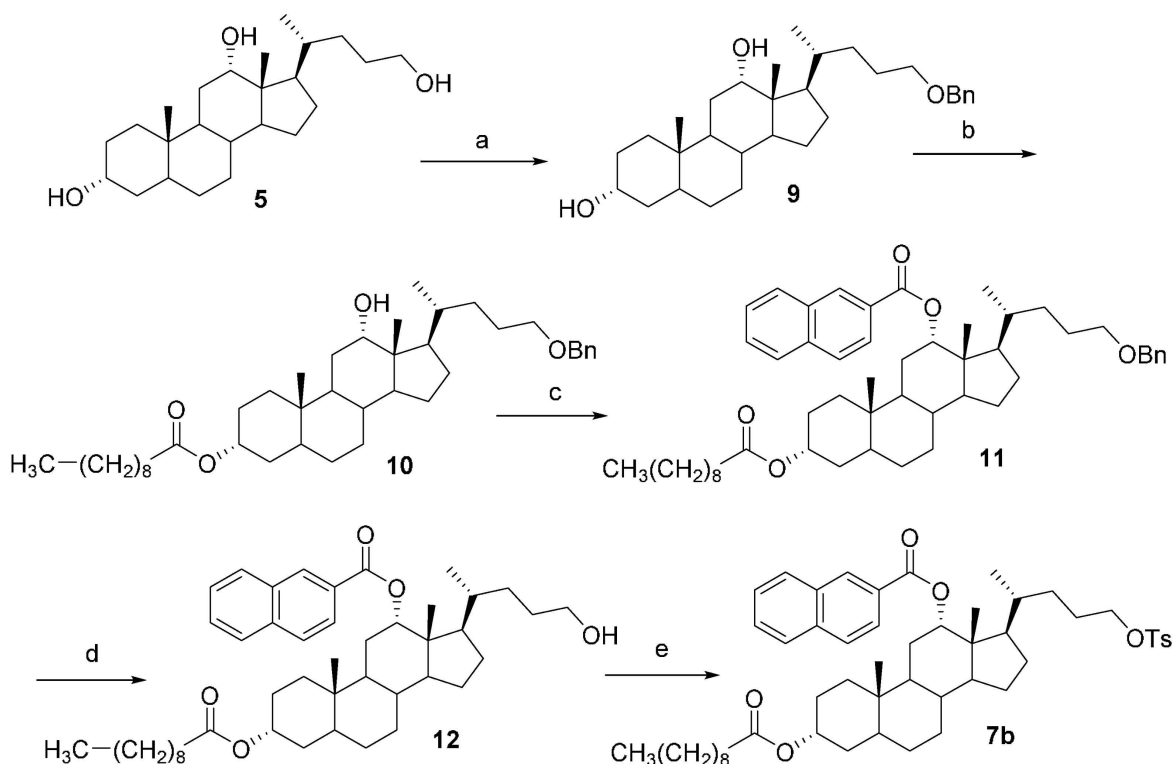
compromise that allowed for the reaction of the axial 12-hydroxyl group and prevented the tosylate displacement.

Derivative **7c** was obtained by exploiting the different reactivity of the two hydroxyl groups. By reacting **6** with 2-naphthoyl chloride in the presence of triethylamine and a catalytic amount of DMAP at room temperature only the equatorial hydroxyl group reacted, affording derivative **8** in a 72% yield, after chromatographic purification. The derivatization of the 12-hydroxyl group under the conditions to obtain **7a** did not afford the desired product, given that the displacement of the tosylate group by the chloride anion took place even at 50 °C. Therefore, to obtain **7c** a different procedure was used and **8** was reacted with undecanoic acid in the presence of DCC and DMAP in dichloromethane solution at room temperature.^[54] Under these conditions **7c** was obtained in a 90% yield, after chromatographic purification.

This synthetic protocol did not succeed in the achievement of **7b**, because the esterification of the 12-hydroxyl group with 2-naphthoic acid in the presence of DCC and DMAP did not work; in addition, the use of naphthoyl chloride afforded the displacement of the tosylate group under various reaction conditions. Therefore, given that the problem was the presence of the tosylate at 24-position, the synthetic strategy was modified, introducing this group at the end of the synthesis

and protecting the primary hydroxyl group of the trihydroxylcholine to prevent its undesired derivatization. The synthetic pathway to obtain **7b** is summarized in Scheme 2. According to the Scheme the primary hydroxyl group of trihydroxylcholine **5** was protected as benzyl ether by reacting **5** with NaH in the presence of BTEAC then adding benzyl bromide. The selectivity of this reaction was not high and benzylether **9** was obtained in moderate yield after chromatographic purification. The two hydroxyl groups of **9** were selectively derivatized simply working at different temperature. The 3-hydroxyl group was converted to decanoyl ester by reacting **9** with decanoyl chloride in the presence of triethylamine at room temperature, whereas the 12-naphthoyl ester was obtained by reacting **10** with 2-naphthoyl chloride and triethylamine in refluxing toluene. These reaction conditions gave **11** in a 67% yield from **9**. The hydrogenolysis of the benzyl group, under standard conditions, and the tosylation of the primary hydroxyl group afforded **7b** in 80% yield (two steps).

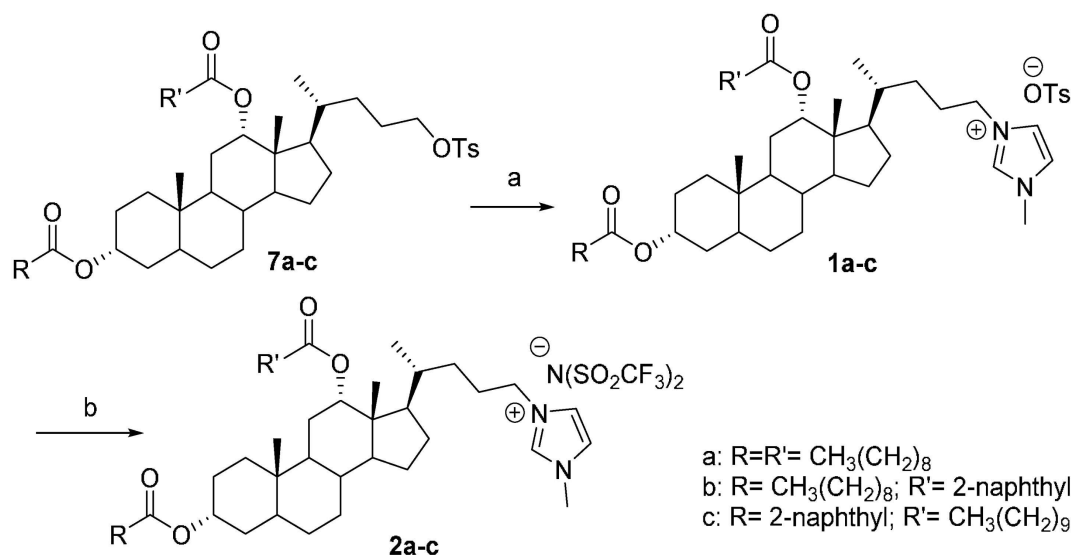
To obtain the ionic compounds, tosylates **7a–c** were reacted with 1-methylimidazole in refluxing acetonitrile, obtaining quantitative yield of liquid ionic compounds **1a–c**. The anion exchange with lithium bis-trifluoromethanesulfonamide gave CILs **2a–c** in quantitative yield (Scheme 3).



Reagents and conditions

a: NaH, BTEAC, THF, 30 min, then BnBr, 24 h; **b:** decanoyl chloride, Et₃N, DMAP, rt, 24 h; **c:** 2-naphthoyl chloride, Et₃N, DMAP, toluene, reflux, 24 h; **d:** H₂, Pd/C, rt, 15 h; **e:** TsCl, Et₃N, rt, 24 h

Scheme 2. Synthesis of tosylate **7b**.

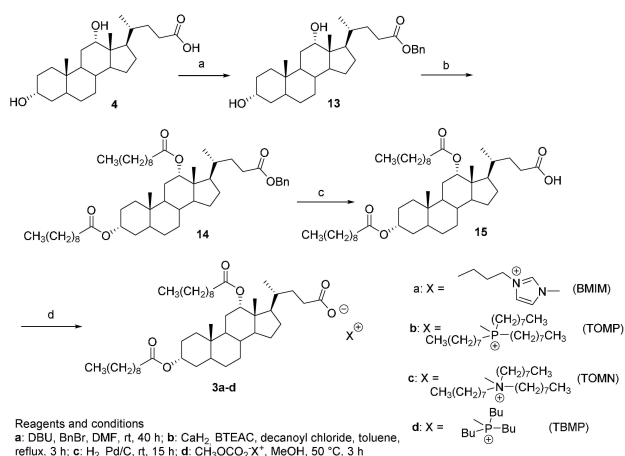


Reagents and conditions

a: N-methylimidazole, acetonitrile, reflux, 48 h; b: lithium bis-trifluoromethanesulfonamide, MeOH, reflux, 48 h

Scheme 3. Synthesis of the CILs 1a–c and 2a–c.

The synthetic pathway to CILs 3a–d, having the chiral steroidal anion, is summarized in Scheme 4. The synthesis of these CILs was shorter and simpler with respect to the previous ones. After protection of the carboxylic acid group as benzylester, the two hydroxyl groups were transformed into the corresponding decanoyl esters under the previously described reaction conditions, by performing the reaction in refluxing toluene: product 14 was obtained in 86% yield after 3 h reaction. Hydrogenolysis of the benzylester, under standard condition, gave 15 in 87% yield. The ionic compounds were eventually obtained in nearly quantitative yields, by reacting 15 with the different methylcarbonate organic salts in methanol solution, according to a reported procedure.^[54]



Scheme 4. Synthesis of CILS 3a–d.

2.2. Thermal Analysis: TGA and DSC Features

The thermal stability of the new CILs has been studied by thermogravimetric (TGA) analysis. The TGA features of all CILs are compared in Figure 2.

The two series of CILs with chiral cations correspond to the blue curves (1a–c with tosylate counter anion) and red curves (2a–c with bistriflimide counter anion). Cases 1a and 2a, featuring both aliphatic (decanoyl) ester groups, have simple patterns consisting in two neat subsequent steps, both of which are significantly shifted to higher temperatures in the case of bistriflimide anions; thus the bistriflimide salt combines in this case its typical advantage of a lower melting point (see next paragraph) with better thermal stability. Less straightforward is the comparative discussion of cases 1b and 2b or 1c and 2c involving a naphthoyl-substituent in two different positions, 12 (axial) in the first case and 3 (equatorial) in the second case, and a long alkyl chain (decanoyl or undecanoyl) in the complementary position. In particular, it seems that the axial ester structure in combination with the anion type plays a great effect. Considering the first degradation event, 1b which is characterized by the naphthoyl ester in position 12 results as the most stable IL. However, when the same cationic moiety is paired with the less nucleophilic Tf₂N anion, the corresponding IL 2b is the least stable IL of the series. Conversely, the more flexible aliphatic ester in the same axial position as well as the naphthoyl group in the usually more stable equatorial position seem to have less impact on the thermal stability, with 1c and 2c showing thermal degradation profiles more similar to 1a and 2a. Therefore, subtle effects of the structure of the axial substituent and of the type (size and nucleophilicity) of the anion can be envisaged in triggering the thermal degradation process.

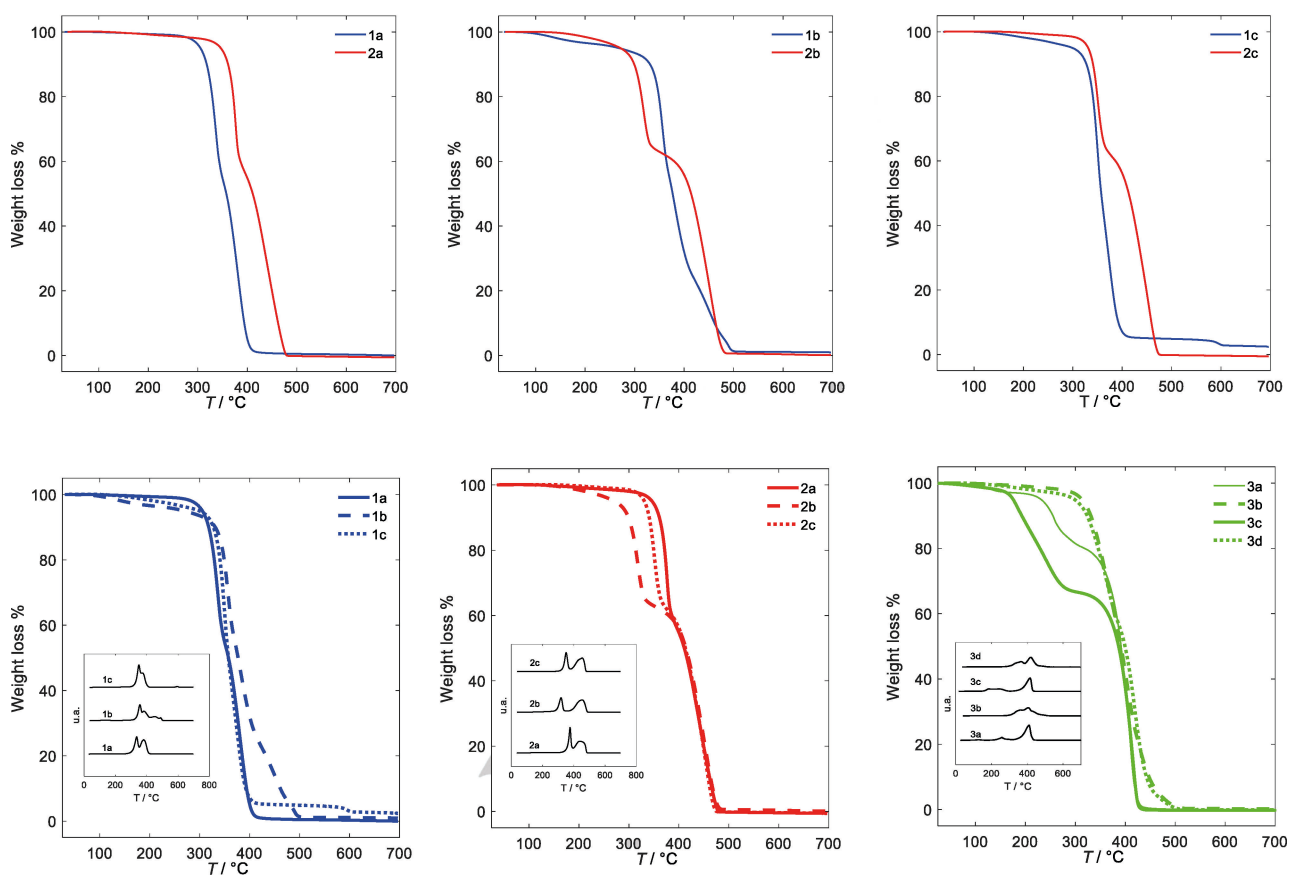


Figure 2. Comparing TGA features of CILs with chiral cations **1 a–c** (blue curves) and **2 a–c** (red curves), as well as of CILs with chiral anions **3 a–d** (green curves); insets provide a comparison of the curve derivatives.

The TGA features of the four CILs **3 a–d** with chiral anions are reported as green curves in Figure 2. They look remarkably modulated by the achiral counterion, in this case a cation, with a clear ammonium < imidazolium < phosphonium stability sequence. In fact, a first step is observed at $\sim 160^\circ\text{C}$ with trioctyl methylammonium (**3 c**), at $\sim 220^\circ\text{C}$ with butyl methylimidazolium cations (**3 a**), and at $\sim 290^\circ\text{C}$ with tributyl methyl- or trioctyl methyl phosphonium cations (**3 b** and **3 d**). Instead a second step, corresponding to the sharper maximum in the first derivative, is nearly coincident in all cases, and can be therefore linked to the common chiral anion moiety. Solid/liquid phase transitions of the new CILs have been studied by differential scanning calorimetry DSC.

The DSC features of the six CILs with chiral cations are reported in Figure SI 47. In all cases, weak but significant features pointing to liquid/solid and solid/liquid reversible glassy transitions can be observed, becoming reproducible from the second cycle, while in the first one they can be significantly different. Such transitions (particularly considering the stationary cycles) appear systematically shifted to lower temperatures with the bistriflimide anion, a well-known tool promoting melting point lowering in IL design. Moreover, notably, changing a long-chain alkyl ester substituent with a naphthyl one results in a remarkable increase of the liquid/solid

transition temperature, even becoming border line respect to room temperature.

The DSC features of the four CILs with chiral anions are reported in Figure SI 48. The glass transitions are in these cases even more difficult to perceive but located at temperatures even lower than former cases **1 a** and **2 a** (which feature the same chiral building block with two decanoyl esters).

2.3. Electrochemical Properties

The electrochemical properties of the new CIL family were investigated by cyclic voltammetry CV in the $0.05\text{--}2\text{ V s}^{-1}$ A potential scan rate range.

A synopsis of CV patterns for the six CILs with chiral cations is reported at Figure 3a. The first reduction peak at $\sim -2.5\text{ V}$ vs $\text{Fc}^+|\text{Fc}$ as well as the oxidation peak at $\sim +1.6\text{ V}$ vs $\text{Fc}^+|\text{Fc}$, which are only featured by couples **1 b/2 b** and **1 c/2 c**, should be ascribed to reduction (approaching chemical reversibility with increasing scan rate, see Figure SI 49) and oxidation of the aromatic naphthyl system, respectively. Instead the second reduction peak at $\sim -3\text{ V}$, also featured by the **1 a/2 a** couple, should be assigned to the reduction of the imidazolium cation (chemically irreversible in the scan rate range considered).

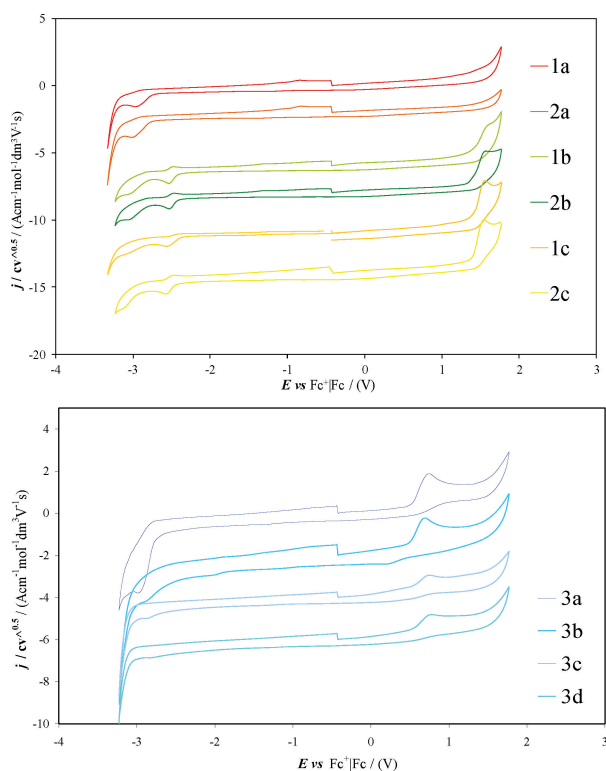


Figure 3. A synopsis of CV features of the six CILs with chiral cations, recorded at 0.2 V s^{-1} scan rate, in $0.00075 \text{ mol dm}^{-3}$ solutions in ACN + TBAPF₆ 0.1 mol dm^{-3} (top) and of CV features of four CILs with chiral anions, recorded at 0.2 V s^{-1} scan rate, in $0.00075 \text{ mol dm}^{-3}$ solutions in ACN + TBAPF₆ 0.1 mol dm^{-3} (bottom). Potentials have been normalized vs the formal potential of the intersolvental ferricenium | ferrocene (Fc⁺ | Fc) reference redox couple, recorded in the same conditions.

Overall, these CILs offer large potential windows for electroanalysis and electrochemistry, both on the oxidation and reduction sides, particularly in the **1 a/2 a** cases ($\sim 4.6 \text{ V}$), but even in the **1 b/2 b** and **1 c/2 c** ones ($\sim 3.7 \text{ V}$).

A synopsis of CV patterns for the four CILs with chiral anions is reported at Figure 3b (while Figure SI 50 shows the effect of scan rate on selected CV peaks).

A reduction peak at $\sim -3 \text{ V}$, analogous to those observed in the former cases, is perceivable for **3 a** only, consistently with it being the only CIL in the **3 a–3 d** group including an imidazolium cation. Instead the oxidation peak at $\sim 0.8 \text{ V vs Fc}^+ | \text{Fc}$ can be ascribed to the oxidation of the carboxylate anion. In fact, its potential is consistent with that observed in ACN for the oxidation of tetrabutylammonium acetate on glassy carbon GC in acetonitrile in non-catalytic conditions.^[55]

2.4. Enantiodiscrimination Tests

The CIL enantiodiscrimination ability has been tested in CV experiments with (*R*)-(+)- or (*S*)-(–)-*N,N*-dimethyl-1-ferrocenylethylamine (*R*)-Fc and (*S*)-Fc, the enantiomers of our benchmark chiral electroactive model probe, commercially available and resulting in chemically and electrochemically reversible canon-

ical CV peaks at mild potentials, well within the potential windows of the current tested media.

The chiral salts were tested as 0.05 mol dm^{-3} chiral additives in bulk BMIMTf₂N, recording in the resulting media the CV patterns of (*R*)-Fc and (*S*)-Fc at 0.05 V s^{-1} scan rate in open air on laboratory screen printed electrode (SPE) cells on plastic sheet, including graphite working and counter electrodes and Ag pseudo-reference electrode, resulting in good reproducibility at constant conditions with the present working protocol. Addition of a small volume of aqueous KCl solution 0.1 mol dm^{-3} to the chiral medium enabled to stabilize the potential of the pseudo-reference electrode, besides advantageously resulting in lower viscosity. Repetitions on new SPE supports were performed in order to check the result repeatability.

As shown in Figure 4a (salts with chiral cations) and Figure 4b (salts with chiral anion), statistically significant differences, of the order of several tens of mV, are observed in all cases for the formal potentials of the ferrocenyl probe enantiomers. In the case of the additives with chiral cations:

- i) The signals of the ferrocenyl probes maintain canonical reversibility features.
- ii) The sequence of activation of the chiral probes is (*R*)- before (*S*)- in all cases; this is consistent with chirality originating from the same chiral steroid building block in all the chiral salts considered.
- iii) However, at constant sequence of probe enantiomer CV peaks, the achiral anions appear to modulate enantio-discrimination; in particular, peak potential differences look systematically larger with NTF₂ anion respect to the OTs one.
- iv) In the case **2 c** a test about additive concentration effect is also provided, resulting in increasing enantiomer potential differences at increasing additive concentrations.

Significant peak potential differences were also observed with the additives with chiral anions, again with the same enantiomer peak order (consistently with the anion chirality originating from the same steroid building block) slightly modulated by the achiral cation. Notably, working in the concurrent presence of carboxylate and ferrocene groups, complications could be expected. In fact, it has been shown that ferrocene can act as a mediator for carboxylate oxidation, which thus shifts to a much lower potential, namely that of ferrocene oxidation; this is evidenced by the ferrocene oxidation peak increasing in current and becoming chemically irreversible.^[56] However, very conveniently, in our case the ferrocene oxidation CV peaks remain canonical, pointing to the above process not taking place (at least significantly). Actually it should be considered that the cited literature study (a) has been performed in acetonitrile, and the mechanism proposed for the follow up of the charge transfer process involves addition of acetonitrile; (b) consider acetate or benzoate salts, which form methyl or benzyl radicals and then carbocations, which are likely to be much more reactive than in our case. We also verified that performing the same protocol in achiral BMIMTf₂N in the absence of the chiral additive, the (*R*)- and (*S*)-probe enantiomers give practically coincident peak potentials (Figure SI 51).

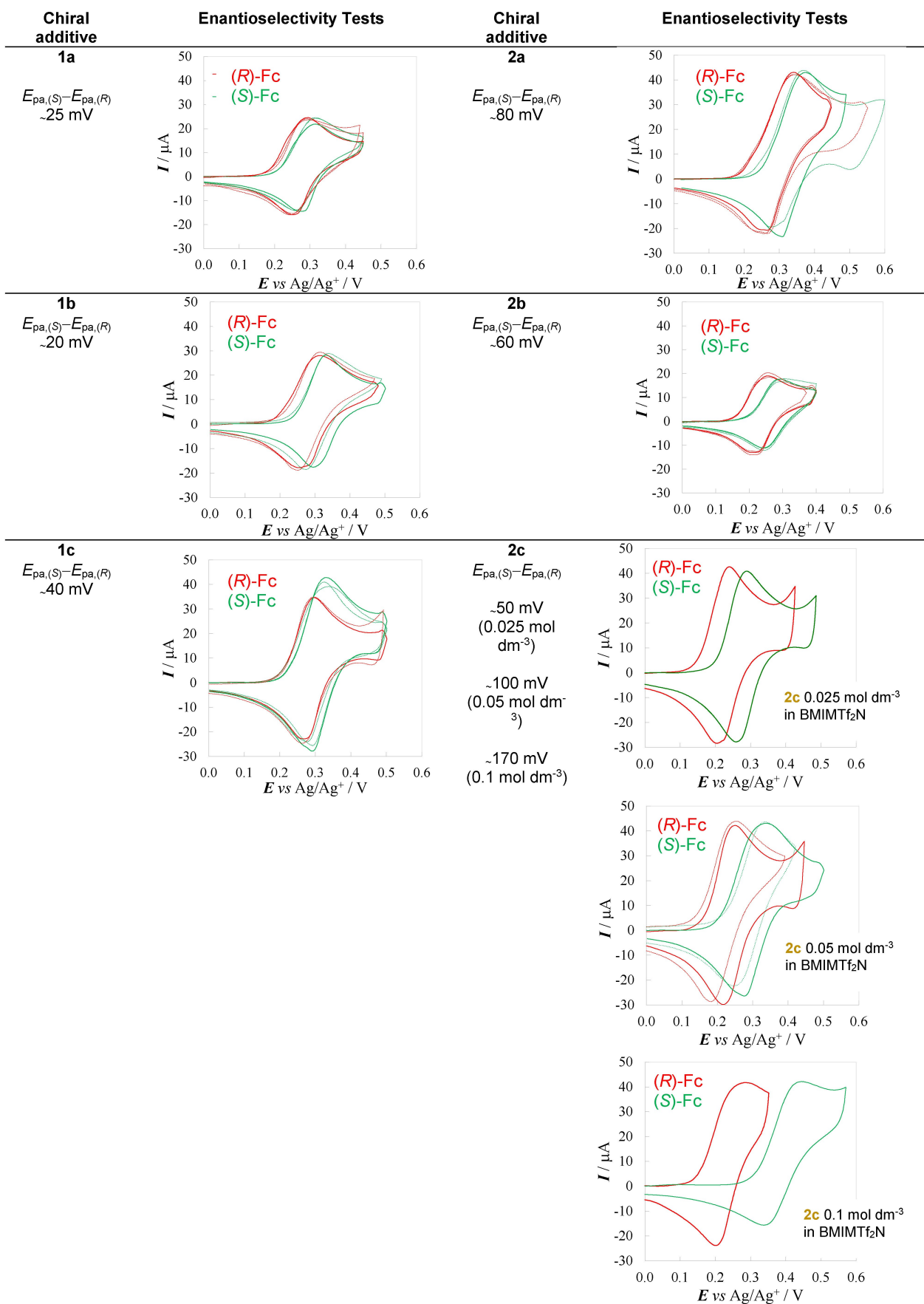


Figure 4a. Enantiodiscrimination tests with (S)- or (R)- ferrocenyl chiral probes (green and red respectively), using the CBILs with chiral cation as low concentration chiral additives (0.05 mol dm⁻³) in commercial IL. For compound 2c a series of enantioselection tests is also provided at increasing CBIL concentration in the 0.025–0.1 mol dm⁻³ range. Repetition tests are also reported (thin lines).

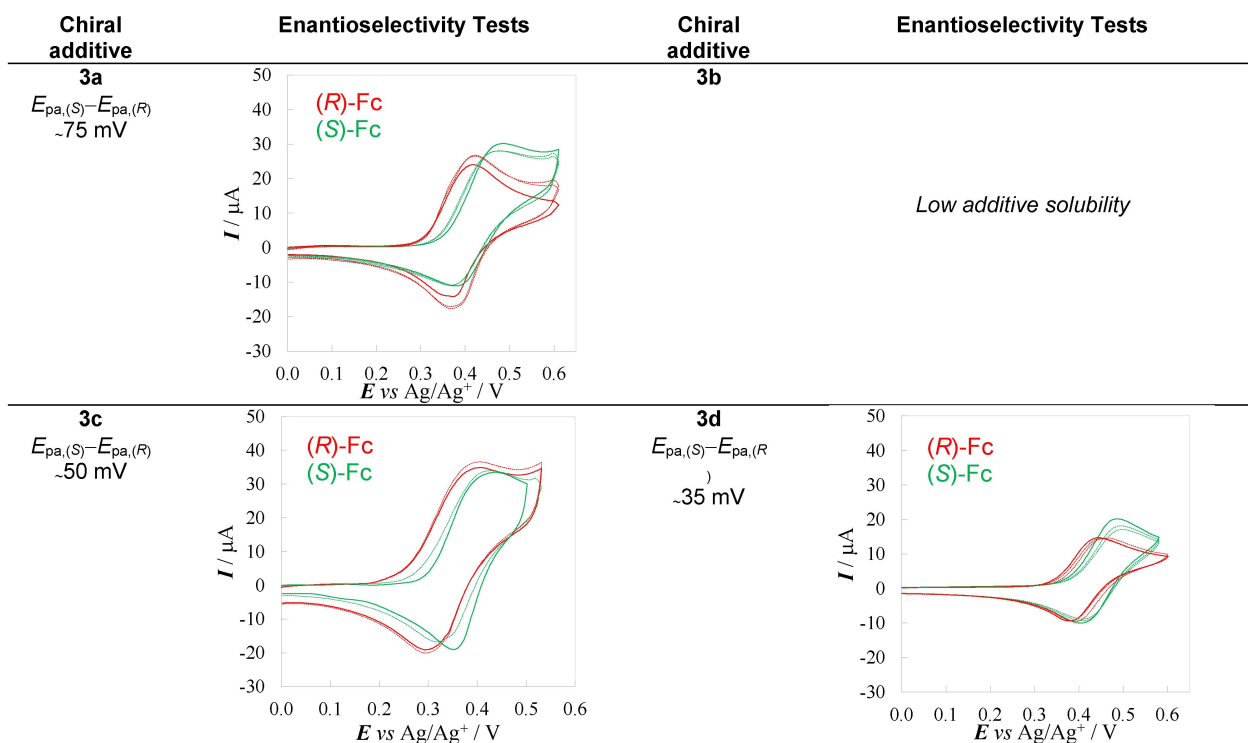


Figure 4b. Enantiodiscrimination tests with (S)- or (R)- ferrocenyl chiral probes (green and red respectively), using the CBILs with chiral anion as low concentration chiral additives. Repetition tests are also reported (thin lines).

3. Conclusions

A novel family of biobased molecular salts with CIL properties has been developed, implementing the chiral steroid building block of the deoxycholic acid, including several stereogenic centers of established absolute configuration, either in the salt anion or cation.

The new salts, although quite viscous, appear liquid at (or close to) room temperature and stable in a wide temperature range; moreover, they offer wide potential windows, useful for both oxidative and reductive experiments in chiral electroanalysis and electrochemistry, a still unexplored field for bile-acid based chiral selectors.

A successful first series of enantiodiscrimination tests were performed recording on disposable SPE cells the cyclic voltammetry features of the enantiomers of a model electroactive chiral probe. While in achiral ionic liquid the probe enantiomers gave of course equivalent CV response, in the presence of moderate amounts of the bile-acid based molecular salts as additives significant potential differences were observed, in the same enantiomer sequence (accordingly to all selectors having the same chiral building block configuration), slightly modulated by the salt achiral counterions.

Such proof-of-concept observations widen the application fields of bile acid derivatives as chiral selectors, while symmetrically enriching the still very few CIL families so far explored for application in chiral electrochemistry and electroanalysis.

Experimental Section

CILs Synthesis and Characterization

All the reactions involving sensitive compounds were carried out under dry Ar, in flame-dried glassware. Dry toluene was obtained by refluxing the commercial toluene over Na/Benzophenone followed by distillation under Ar. Triethylamine was distilled from CaH₂. If not noted otherwise, reactants and reagents were commercially available and used as received from Fluorochem, TCI-Chemicals, Sigma-Aldrich, and Acros Organics.

TLC analyses were carried out with Merck 60 F254 plates (0.2 mm).

The ¹H NMR spectra were recorded in CDCl₃ on a Bruker 400 MHz NMR spectrometer or a Varian Gemini 200 spectrometer or a Bruker AC-250. The following abbreviations are used: s=singlet, d=doublet, dd=double doublet, dt=double triplet, t=triplet, td=triple doublet, q=quartet, m=multiplet, br s= broad signal. ¹³C NMR spectra were recorded at 101 MHz or 62.5 MHz. ¹H and ¹³C NMR chemical shifts (ppm) are referred to TMS as external standard.

Elemental analyses were obtained using an Elementar Vario MICRO cube equipment.

Optical rotations were measured in 1 dm cells at the sodium D line, using a Jasco DIP 360 polarimeter. Melting points were measured using a Büchi Melting Point B-545.

TGA Analysis

The thermal degradation of the synthesized CBILs was investigated by thermal gravimetric analysis (TA Instruments Q500 TGA). The instrument was calibrated using weight standards (1 g and 100 mg) and the temperature calibration was performed using a curie

temperature of nickel standard. All the standards were supplied by TA Instruments Inc. The sample (10–15 mg) was heated at 40 °C in a platinum crucible for the drying procedure and maintained in N₂ flow (90 mL min⁻¹) for 30 min. Then, CBIL was heated from 40 °C to 700 °C with a heating rate of 10 °C min⁻¹ under nitrogen (90 mL min⁻¹) and maintained at 700 °C for 3 min. Mass change was recorded as a function of temperature and time. TGA experiments were carried out in duplicate.

DSC analysis have been performed by a DSC 3500 STARe system from Mettler-Toledo® equipped with a HUBER TC100-MTcooler, on a few mg of CILs (weighed on a high-precision balance) in pin-holed standard aluminum crucibles (No. 00026763, 40 mm³). Weight constancy between room temperature and 200 °C has been verified by a combined TGA/DSC 3 STARe system from Mettler-Toledo®, in standard alumina crucibles (No. 00024123, 70 mm³), under the same nitrogen flux. DSC thermograms were acquired at 10 °C min⁻¹ scan rate, in nitrogen flow (50 cm³ min⁻¹), according to the following temperature program: cooling from 25 °C to -85 °C; heating from -85 °C to 200 °C; cooling from 200 °C to -85 °C; heating from -85 °C to 25 °C; cooling from 25 °C to -85 °C; heating from -85 °C to 200 °C.

Electrochemical Characterization

The ten CBILs were electrochemically characterized by cyclic voltammetry CV at scan rates ranging 0.05–2 V s⁻¹ using an AutoLab PGStat potentiostat and a classical three-electrode glass minicell (working volume about 3 cm³). The latter included as working electrode a glassy carbon GC disk (Metrohm, S=0.072 cm²) polished by diamond powder (1 μm Aldrich) on a wet cloth (Struers DP-NAP), as counter electrode a platinum disk, and as reference electrode a saturated aqueous calomel one (SCE) inserted in a compartment with the working medium ending in a porous frit, to avoid contamination of the working solution by water and KCl traces. Experiments were run on 0.00075 mol dm⁻³ solutions in ACN + 0.1 mol dm⁻³ tetrabutylammonium hexafluorophosphate TBAPF₆ as the supporting electrolyte, previously deaerated by nitrogen bubbling. Positive and negative half cycles have been separately recorded to avoid reciprocal contamination by electron transfer products. The reported potentials have been normalized vs the formal potential of the intercalated ferricinium|ferrocene (Fc⁺|Fc) reference redox couple, recorded in the same conditions.

Enantiodiscrimination CV Tests

CV enantioselectivity tests were performed by cyclic voltammetry at 0.05 V/s scan rate on using screen-printed electrode cells (SPE) constituted of working, counter, and Ag/AgCl pseudo-reference electrodes. The electrodes were produced in foils of 48 using screen-printing machine DEK 245 (Weymouth, UK) and flexible polyester film (Autostat HT5) as support obtained from Autotype Italia (Milan, Italy). Graphite-based ink (Elettrodag 421) from Acheson (Milan, Italy) was used to print the working and the counter electrode while silver/silver chloride ink was used to print the reference electrode (Acheson Elettrodag 4038 SS). The diameter of the SPE working electrode was 0.4 cm resulting in an apparent geometric area of 0.126 cm². The experiments were performed using CBILs as low-concentration chiral additives (0.05 mol dm⁻³) in achiral commercial IL 1-butyl-3-methylimidazolium bis(trifluoromethanesulfonyl)imide BMIMTf₂N (or BMIMTFSI; CAS 174899-83-3; Aldrich ≥ 98%). CVs were recorded in open air conditions, depositing on the working electrode a drop of one of the above chiral media with 0.002 mol dm⁻³ (R)-(+)- or (S)-(-)-N,N'-dimethyl-1-ferrocenylethylamine (Aldrich, submitted to a further chromatographic purification step) as the enantiopure probe,

already adopted as model one (on account of its chemical and electrochemical reversibility). For the sake of comparison, the tests were also carried out with the same protocol, but in the absence of the chiral additives. Statistical tests for peak potentials were performed by repeatedly recording the CV pattern of each enantiopure probe, at constant working protocol. In all cases a small volume (6 μL) of aqueous KCl solution 0.1 mol dm⁻³ was added to the chiral medium, to stabilize the potential of the pseudo-reference electrode, besides advantageously resulting in lower viscosity.

Acknowledgements

Support of Fondazione Cariplo and Regione Lombardia (2016-0923 RST – Avviso congiunto FC-RL Sottomisura B) rafforzamento (Enhancing VINCE (Versatile INherently Chiral Electrochemistry)) and of Università degli Studi di Milano are gratefully acknowledged, as well as advanced facilities available at SmartMatLab at Department of Chemistry, Università degli Studi di Milano, operated by Dr. Serena Cappelli, and preliminary CV investigations by Dr. Serena Arnaboldi. Sara Cantucci is also acknowledged for the TOC drawing.

Conflict of Interest

The authors declare no conflict of interest.

Keywords: chiral molecular liquids · chiral molecular salts · ionic liquids · enantiodiscrimination · chiral voltammetry

- [1] S. K. Singh, A. W. Savoy, *J. Mol. Liq.* **2020**, *297*, 1–23.
- [2] T. Welton, *Biophys. Rev. Lett.* **2018**, *10*, 691–706.
- [3] C. P. Kapnissi-Christodoulou, I. J. Stavrou, M. C. Mavroudi, *J. Chromatogr. A* **2014**, *1363*, 2–10.
- [4] B. Karimi, M. Tavakolian, M. Akbari, F. Mansouri, *ChemCatChem* **2018**, *10*, 3173–3205.
- [5] A. Singh, H. Kumar Chopra, *Curr. Org. Synth.* **2017**, *14*, 488–510.
- [6] A. C. Gaumont, Y. Génisson, F. Guillen, V. Zgonnik, J. C. Plaquevent, *Catal. Methods Asymmetric Synth. Adv. Mater. Tech. Appl.* **2011**, 323–344.
- [7] T. Payagala, D. W. Armstrong, *Chirality* **2012**, *24*, 17–53.
- [8] S. Rizzo, S. Arnaboldi, V. Mihalj, R. Cirilli, A. Forni, A. Gennaro, A. A. Isse, M. Pierini, P. R. Mussini, F. Sannicolò, *Angew. Chem.* **2017**, *56*, 2079–2082.
- [9] M. Longhi, S. Arnaboldi, E. Husanu, S. Grecchi, I. F. Buzzi, R. Cirilli, S. Rizzo, C. Chiappe, P. R. Mussini, L. Guazzelli, *Electrochim. Acta* **2019**, *298*, 194–209.
- [10] S. Rizzo, S. Arnaboldi, R. Cirilli, A. Gennaro, A. A. Isse, F. Sannicolò, P. R. Mussini, *Electrochem. Commun.* **2018**, *89*, 57–61.
- [11] F. Fontana, B. Bertolotti, P. R. Mussini, S. Arnaboldi, S. Grecchi, R. Cirilli, L. Micheli, S. Rizzo, *Molecules* **2021**, *26*, 311 (13 pages).
- [12] M. Z. Bazant, B. D. Storey, A. A. Kornishev, *Phys. Rev. Lett.* **2011**, *106*, 046102/1–046102/4.
- [13] S. Perkin, L. Crowhurst, H. Niedermeyer, T. Welton, A. A. Smith, N. N. Goswami, *Chem. Commun.* **2011**, *47*, 6572–6574.
- [14] V. Ivaništšev, S. O'Connor, M. V. Fedorov, *Electrochem. Commun.* **2014**, *48*, 61–64.
- [15] V. Ivaništšev, K. Kirchner, M. V. Fedorov, *J. Phys. Condens. Mater.* **2015**, *27*, 102101/1–102101/5.
- [16] R. Hayes, G. G. Warr, R. Atkin, *Chem. Rev.* **2015**, *115*, 6357–6426.
- [17] K. Ma, R. Jarosova, G. M. Swain, G. J. Blanchard, *Langmuir* **2016**, *32*, 9507–9512.

- [18] T. Cui, A. Lahiri, T. Carstens, N. Borisenko, G. Pulletikurthi, C. Kuhl, F. Endres, *J. Phys. Chem. C* **2016**, *120*, 9341–9349.
- [19] T. Zhong, J. Yan, M. Li, L. Chen, B. Ma, *ChemElectroChem* **2016**, *3*, 2221–2226.
- [20] J.-W. Yan, Z.-Q. Tian, B.-W. Mao, *Curr. Opin. Electrochem.* **2017**, *4*, 105–111.
- [21] Y. Wang, R. Jarošová, G. M. Swain, G. J. Blanchard, *Langmuir* **2020**, *36*, 3038–3045.
- [22] J. P. de Souza, Z. A. H. Goodwin, M. McEldrew, A. A. Kornyshev, M. Z. Bazant, *Phys. Rev. Lett.* **2020**, *125*, 116001 (6 pages).
- [23] S. Watanabe, G. A. Pilkington, A. Oleshkevych, P. Pedraz, M. Radiom, R. Welbourn, S. Glavatskih, M. W. Rutland, *Phys. Chem. Chem. Phys.* **2020**, *22*, 8450–8460.
- [24] Y. Wang, F. Parvis, Md. Iqbal Hossain, K. Ma, R. Jarosova, G. M. Swain, G. J. Blanchard, *Langmuir* **2021**, *37*, 605–615.
- [25] N. Katsonis, E. Lacaze, A. Ferrarini, *J. Mater. Chem.* **2012**, *22*, 7088–7097.
- [26] Preliminary data still to be published.
- [27] L. Vaton-Chanvrier, V. Peulon, Y. Combret, C. J. Combret, *Chromatographia* **1997**, *46*, 613.
- [28] T. Takeuchi, J. Chu, T. Miwa, *Chromatographia* **1998**, *47*, 183.
- [29] L. Vaton-Chanvrier, H. Oulyadi, Y. Combret, G. Coquerel, J. Combret, *Chirality* **2001**, *13*, 668–674.
- [30] A. Iuliano, G. Félix, *J. Chromatogr. A* **2004**, *1031*, 187–195.
- [31] A. Iuliano, P. Scafato, *Tetrahedron: Asymmetry* **2003**, *14*, 611–618.
- [32] A. Iuliano, P. Scafato, R. Torchia, *Tetrahedron: Asymmetry* **2004**, *15*, 2533–2538.
- [33] G. L. Puleo, M. Masi, A. Iuliano *Tetrahedron: Asymmetry* **2007**, *18*, 1364–1375.
- [34] V. R. Jumde, A. Iuliano, *Adv. Synth. Catal.* **2013**, *355*, 3475–3483.
- [35] V. Zullo, A. Iuliano, *Eur. J. Org. Chem.* **2019**, 1377–1384.
- [36] U. Maitra, P. Mathivanan, *J. Chem. Soc. Chem. Commun.* **1993**, 1469–1471.
- [37] P. Mathivanan, U. Maitra, *J. Org. Chem.* **1995**, *60*, 364–369.
- [38] U. Maitra, A. K. Bandyopadhyaya, N. M. Sangeetha, *J. Org. Chem.* **2000**, *65*, 8239–8244.
- [39] S. Caporali, C. Chiappe, T. Ghilardi, A. Iuliano, G. Longhi, P. Margari, C. S. Pomelli, *RSC Adv.* **2016**, *6*, 8053–8060.
- [40] A. Mezzetta, J. Łuczak, J. Woch, C. Chiappe, J. Nowicki, L. Guazzelli, *J. Mol. Liq.* **2019**, *289*, 111155.
- [41] C. Chiappe, P. Margari, A. Mezzetta, C. S. Pomelli, S. Koutsoumpos, M. Papamichael, P. Giannios, K. Moutzouris, *Phys. Chem. Chem. Phys.* **2017**, *19*, 8201–8209.
- [42] S. Becherini, A. Mezzetta, C. Chiappe, L. Guazzelli, *New J. Chem.* **2019**, *43*, 4554–4561.
- [43] A. Mezzetta, V. Perillo, L. Guazzelli, C. Chiappe, *J. Therm. Anal. Calorim.* **2019**, *138*, 3335–3345.
- [44] A. Iuliano, P. Salvadori, G. Félix, *Tetrahedron: Asymmetry* **1999**, *10*, 3353–3364.
- [45] A. Iuliano, G. Masini, P. Salvadori, G. Félix, *Tetrahedron: Asymmetry* **2001**, *12*, 2811–2825.
- [46] A. Iuliano, D. Losi, S. Facchetti, *J. Org. Chem.* **2007**, *72*, 8472–8477.
- [47] A. Iuliano, S. Facchetti, T. Funaioli, *Chem. Commun.* **2009**, 457–459.
- [48] S. Facchetti, I. Cavallini, T. Funaioli, F. Marchetti, A. Iuliano, *Organometallics* **2009**, *28*, 4150–4158.
- [49] V. R. Jumde, S. Facchetti, A. Iuliano, *Tetrahedron: Asymmetry* **2010**, *21*, 2775–2781.
- [50] G. Iannucci, A. Iuliano, *J. Organomet. Chem.* **2016**, *806*, 88.
- [51] A. Passera, A. Iuliano, J. J. Pérez-Torrente, V. Passarelli, *Dalton Trans.* **2018**, *47*, 2292–2305.
- [52] S. Bhat, U. Maitra, *Tetrahedron* **2007**, *63*, 7309–7320.
- [53] Mrozek, L. Dvokarova, Z. Mandelova, L. Rarova, A. Rezacova, L. Placek, R. Opatrilova, J. Dhonal, O. Paleta, V. Kral, P. Drasal, J. Jampilek, *Steroids* **2011**, *76*, 1082–1097.
- [54] B. Sellergren, J. Wieschenmeyer, K. S. Boos, D. Seidel, *Chem. Mater.* **1998**, *10*, 4037–4046.
- [55] L. Guglielmero, A. Mezzetta, C. S. Pomelli, C. Chiappe, L. Guazzelli, *J. CO₂ Util.* **2019**, *34*, 437–445.
- [56] L. S. Hernández-Muñoz, A. Galano, P. D. Astudillo-Sánchez, M. M. Abu-Omar, F. González, *Electrochim. Acta* **2014**, 136.

Manuscript received: February 12, 2021

Revised manuscript received: March 4, 2021

Accepted manuscript online: March 12, 2021